Preliminary Sensitivity Analysis of Control Rod Absorber Materials on the Chemical Speciation of Fission Products during a Severe Accident

Dowoong Hwang [a,b], Serin Kim [a,b], Yoonhee Lee [a*]
[a]*Dept. of Energy Engineering, Korea Institute of Energy Technology,*
21 Kentech-gil, Naju-si, Jeonnam State 58330, Republic of Korea
[b]*Dept. of Applied Plasma and Quantum Beam Engineering, Jeonbuk National University,*
567, Baekje-daero, Deokjin-gu, Jeonju, Jeonbuk State, Korea 54896
**Corresponding author: yooney@kentech.ac.kr*

***Keywords :** Source term, Fission products, Control rod, Serpent 2, GEMS

1. Introduction

The best estimate analysis requires reliable chemical forms of the fission products released to the containment of a nuclear power plant, since the radiation dose depends on their physicochemical forms.

Numerous works have been performed for conventional light water reactors [1, 2], and it has been recognized that the chemical forms of fission products are affected not only by an accident sequence but also by reactor core designs.

The challenge is further compounded by innovative SMR concepts such as the i-SMR, which employs two types of control rods in a single reactor core; Silver-Indium-Cadmium (SIC) control rods are used for the regulating bank, whereas Boron-Carbide (B_4C) control rods are used for the shutdown bank [3]. Such a configuration has never been implemented in any commercial reactors. As discussed previously, the chemical forms of fission products are influenced by the type of control rod absorber, therefore, it is necessary to evaluate the impact of the aforementioned control rod configuration in the i-SMR on the chemical forms of fission products under severe accident conditions.

In this work, as an initial step toward assessing the impact of the aforementioned configurations on fission product speciation, a preliminary sensitivity analysis of control rod materials on the chemical speciation of fission products during a severe accident is performed. The analysis is conducted through modifications to the GEMS [4] library, as well as through the coupling of Serpent 2 [5] and GEMS, as established by the authors in previous work [6].

2. Coupling Scheme of Serpent 2 & GEMS

2.1 Numerical Methods in GEMS

In GEMS, chemical speciation is determined by finding the equilibrium state of a multicomponent, multiphase system through minimization of Gibbs energy. GEM framework uses Independent Components (ICs) and Dependent Components (DCs). The speciation vector of DC amounts is obtained by minimizing the total Gibbs energy expressed as Eq. (1)

$$\min_{n>0}\{G(T,P,n)\}\ s.t.\ An=b, \tag{1}$$

where A is the stoichiometric matrix, and b is the vector of total IC amounts and $s.t.$ stands for subject to, indicating the mass balance constraint $An=b$ The Gibbs energy evaluated as a phase-wise sum over DCs,

$$G(T,P,n)=\sum_j\left(n_j\cdot\bar{\mu}_j\right), \tag{2}$$

with the dimensionless chemical potential expressed as

$$\bar{\mu}_j=\frac{G_j^o(T,P)}{R\cdot T}+\ln a_j+AT \tag{3}$$

where G_j° is the standard molar Gibbs energy from the database (with T , P corrections as applicable), R is the universal gas constant, T is temperature and a_j is defined consistently with the phase standard state and the selected activity or equation of state model. Here, AT denotes additional model dependent terms applied for scaling and/or electrostatic contributions and etc.

For the numerical solution, GEMS utilizes interior-point method-3 (IPM-3) in which primal DC amounts and dual IC chemical potentials are solved consistently. Convergence is controlled by user-defined tolerances, including the Dikin's criterion [7] and the admissible IC mass-balance residuals [8].

2.2 Preparation of GEMS Inputs and Extension of HERACLES-TDB

Fig. 1 shows coupling scheme of Serpent 2 and GEMS which the authors have established in previous work [6].

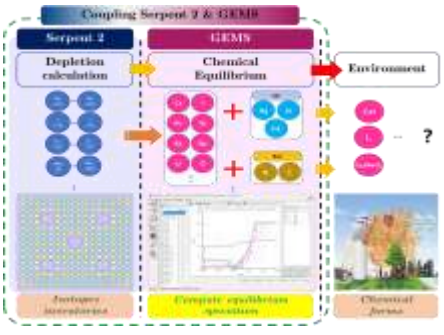

Fig. 1. Coupling scheme of Serpent 2 and GEMS to obtain chemical speciation of the fission products.

Using Serpent 2 depletion calculations, fuel inventories are obtained at selected burnup steps [5], post-processed into elemental molar vectors, and mapped to the GEMS bulk composition input.

In the present study, the chemical system is further extended to explicitly account for the effects of neutron absorber materials in the control rods on the chemical speciation during a severe accident. In addition to the elemental inventory derived from the fuel depletion, absorber-related elemental inputs corresponding to the B_4C and SIC control rod systems are included in the GEMS bulk composition to represent their potential participation in severe-accident chemistry.

Based on thermochemical data listed in Ref. [9], the DC list is further extended because the conventional HERACLES-TDB does not consider absorber-related species required for the present comparison between the B_4C-loaded and SIC-loaded cases properly. Since the GEMS Gibbs-energy-minimization framework predicts the stable equilibrium phase assemblage and speciation for a given bulk composition at specified temperature and pressure, the species extension is designed to represent absorber-related pure substances and major secondary species relevant to interactions with released fission-product elements under severe-accident conditions.

Accordingly, DC entries for $Ag_{(s,l,g)}$, $In_{(s,l,g)}$, $Cd_{(s,l,g)}$, and $B_{(s,l,g)}$, together with associated chemical species relevant to the present SIC/B_4C comparison, such as $AgI_{(s,l,g)}$ and $CsBO_{2(s,l,g)}$, are incorporated into the extended HERACLES-TDB. The resulting dataset is then used consistently in all GEMS equilibrium calculations in this work.

3. Numerical Results

A depletion calculation for typical PWR fuel assembly is performed with Serpent 2 to obtain isotopic inventories with burnup of 52.25 MWd/kgU. The inventories are then used as input for GEMS calculations with the extended HERACLES-TDB [10]. To reflect control rod absorber materials potentially present during a severe accident, absorber-related elements for the SIC and B_4C systems are additionally included, and the resulting temperature-dependent equilibrium speciation is compared. The equilibrium calculations are performed over the temperature range of 800–2,000°C at a fixed pressure of 20 bar. The selected temperature range is intended to examine absorber-dependent speciation trends over a broad high-temperature regime relevant to fission-product release and absorber-material interactions in the reactor core during a severe accident, following depressurization under typical severe accident management guidelines. The computational conditions for Serpent 2 are shown in Table 1, and the gas-phase fractions of fission products for the SIC-loaded and B_4C-loaded cases are presented in Figs. 4 and 5, respectively.

Table 1. Computation conditions in Serpent 2

Parameter		Value
Cross section library		Continuous energy ENDF/B-VII libraries
# of histories		100,000
# of cycles	Inactive	500
	Active	1,000

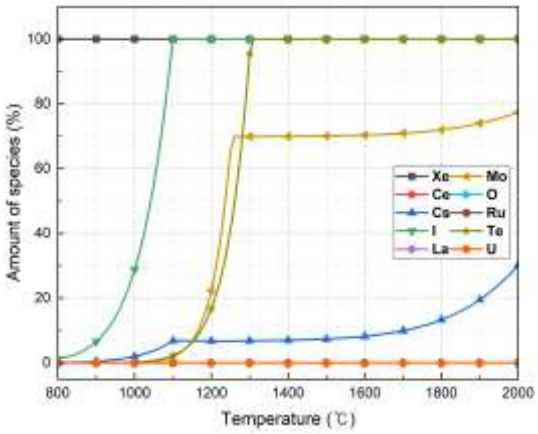

Fig. 4. Gas phase fraction of fission product compounds with SIC at various temperatures.

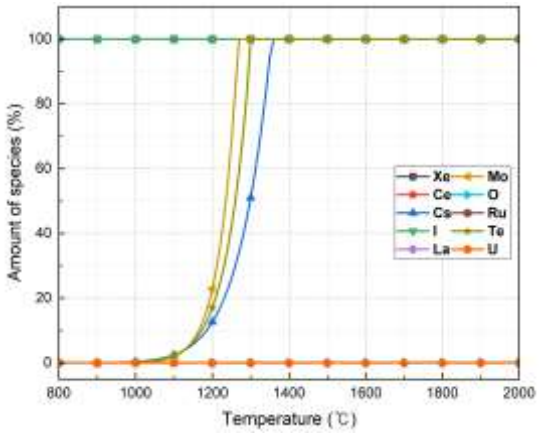

Fig. 5. Gas phase fraction of fission product compounds with B_4C at various temperatures.

As shown in Figs. 4 and 5, for iodine, complete volatilization occurs at substantially different temperatures: in the SIC case the gas-phase fraction reaches 100% at 1,000°C, whereas in the B_4C case iodine is already 100% in the gas phase over the entire temperature range investigated. Molybdenum exhibits incomplete volatilization in the SIC case, reaching 69.8% in the gas phase at 1,260°C and then increasing gradually to 77.4% at 2,000°C; in contrast, in the B_4C case the molybdenum gas-phase fraction rises sharply and reaches 100% at around 1,280°C. Cesium shows the largest absorber-dependent discrepancy: in the SIC case it remains low (6.8% at 1,100°C) and increases

only gradually to approximately 30% at 2,000°C, while in the B_4C case it is present only in trace amounts at 1,000°C but increases rapidly to 51% at 1,300°C and reaches 100% at around 1,360°C.

Figs. 6 and 7 illustrate the equilibrium distribution of iodine compounds over the temperature range considered for the SIC and B_4C control rod absorber cases, respectively.

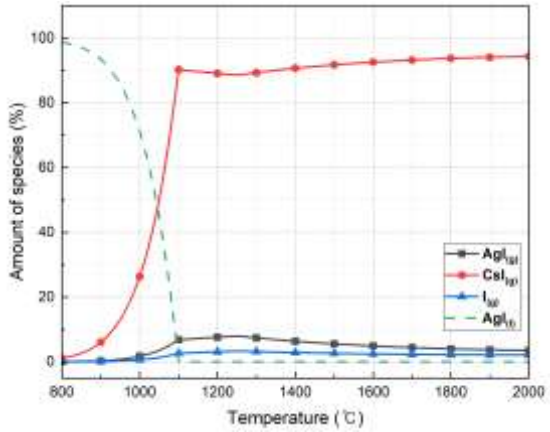

Fig. 6. Fraction of iodine compounds at various temperatures with SIC.

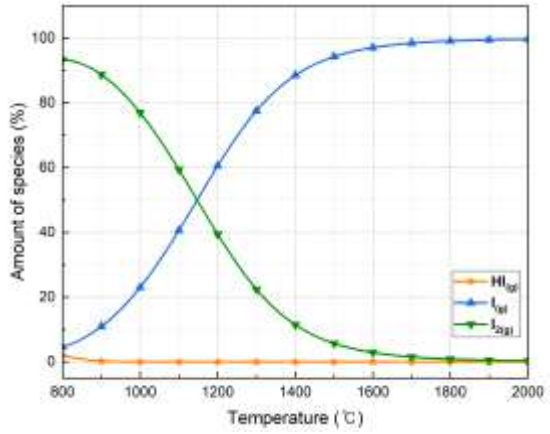

Fig. 7. Fraction of iodine compounds at various temperatures with B_4C.

For iodine-containing species, CsI is the dominant species for SIC-loaded case as shown in Fig. 6; that is, the fraction of CsI accounts for approximately 90% of the iodine species when the temperature exceeds 1,100°C.

In contrast to the SIC-loaded case, molecular and elemental iodine species ($I_{2(g)}$ and $I_{(g)}$) are the dominant species in the B_4C-loaded case as shown in Fig. 7; that is, the combined fraction of these two species accounts for approximately 95% of the iodine species in the gas phase over the entire temperature range considered in this study. The fraction of CsI in this case is significantly lower than that in the SIC-loaded case. The chemical speciation of iodine for the B_4C-loaded case is consistent with the results of the Phebus FP programme, in which the B_4C-loaded test FPT3 exhibited a markedly higher fraction of molecular and elemental iodine compared with the other tests. This behavior is attributed to boron-related chemistry; specifically, the chemical affinity between boron and cesium is significantly higher than that between cesium and iodine [11-13].

Figs. 8 and 9 illustrate the equilibrium distribution of cesium compounds over the temperature range considered for the SIC and B_4C control rod absorber cases, respectively.

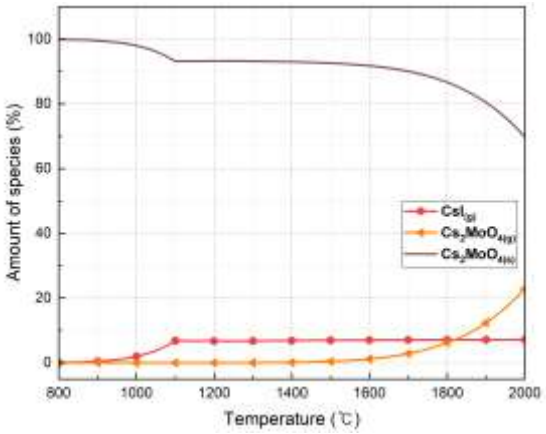

Fig. 8. Fraction of cesium compounds at various temperatures with SIC.

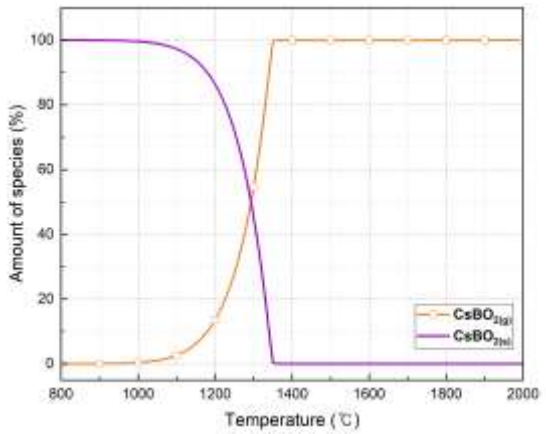

Fig. 9. Fraction of cesium compounds at various temperatures with B_4C.

For cesium-containing species, the condensed phase of Cs_2MoO_4 is the dominant species for SIC-loaded case as shown in Fig. 8; that is, the fraction of Cs_2MoO_4 accounts for approximately 90% of the cesium species when the temperature is less than 1,700°C.

In the case of gas phase of cesium, which is main release form of the cesium during a severe accident, CsI is the dominant species for SIC-loaded case as shown in Fig. 8; that is, the fraction of CsI among the gas phase of cesium accounts for approximately 7% of the cesium

species when the temperature exceeds 1,100°C. The chemical speciation of cesium obtained from the above analysis is consistent with previous studies on MELCOR SOARCA [14].

In contrast to the SIC-loaded case, molecular and $CsBO_2$ are the dominant species in the B_4C-loaded case as shown in Fig. 9; that is, the fraction of the $CsBO_2$ accounts for approximately 100% of the cesium species over the entire temperature range considered in this study. As discussed earlier this behavior is attributed to boron-related chemistry; specifically, the chemical affinity between boron and cesium is significantly higher than that between cesium and iodine [11-13].

4. Conclusions

In this paper, a sensitivity study of the types of control rods absorber materials is performed to evaluate their impact on the speciation of fission products during a severe accident. For this analysis, the HERACLES-TDB library is extended to include the thermochemical data of $Ag_{(s,l,g)}$, $In_{(s,l,g)}$, $Cd_{(s,l,g)}$, and $B_{(s,l,g)}$, as well as their associated chemical species, thereby extending the set of absorber-related pure substances and key secondary phases relevant under severe accident conditions. For iodine-related species in the SIC-loaded case, CsI is the dominant chemical species at temperatures above 1,000°C, whereas in the B_4C-loaded case, elemental and molecular iodine are the dominant species over the entire temperature range considered in this study. For cesium-related species in the SIC-loaded case, CsI is the dominant chemical species at temperatures above 1,000°C, whereas in the B_4C-loaded case $CsBO_2$ is the dominant species over the entire temperature range considered in this study. The aforementioned chemical speciation of iodine and cesium indicates that the absorber material can markedly shift the equilibrium phase partitioning and the physicochemical forms of source-term-relevant elements. This is also consistent with the findings reported in the well-known Phebus FPT experiments.

As future work, HERACLES-TDB will be further extended to include absorber-related thermochemical data, particularly for Cs–Cd–I compounds and other Cd-bearing species reported in the literature, as well as telluride-related species, which are known to be important for determining chemical speciation in the reactor coolant system under severe accident conditions. In addition, this framework will be extended by coupling it with MELCOR to analyze the source term for a severe accident scenario in water-cooled SMRs particularly i-SMR in which the silver-indium-cadmium and boron-carbides are used as neutron absorber materials within a single reactor core.

ACKNOWLEDGEMENTS

This study was supported by the Nuclear Safety Research Program through the Regulatory Research Management Agency for SMRs (RMAS) and the Nuclear Safety and Security Commission (NSSC) of the Republic of Korea. (No. RS-2025-02311309)

REFERENCES

[1] L. Soffer, S. B. Burson, C. M. Ferrell, R. Y. Lee, and J. N. Ridgely, “Accident source terms for light-water nuclear power plants,” NUREG-1465, U.S. Nuclear Regulatory Commission, Feb. 1995.
[2] B. Clément, L. Cantrel, G. Ducros, F. Funke, L. Herranz, A. Rydl, G. Weber, and C. Wren, “State of the art report on iodine chemistry,” NEA/CSNI/R (2007)1, OECD Nuclear Energy Agency, 2007.
[3] W. J. Lee, S. G. Hong, and J. S. Kim, “Neutronic performance evaluation of different control rod materials in soluble boron-free i-SMR core,” in Proc. Trans. Korean Nuclear Society Autumn Meeting, Changwon, Republic of Korea, Oct. 30–31, 2025.
[4] GEM Software (GEMS) Home, http://gems.web.psi.ch/ (visited on Jan. 11, 2025).
[5] J. Leppänen, M. Pusa, T. Viitanen, V. Valtavirta, and T. Kaltiaisenaho, “The Serpent Monte Carlo code: Status, development and applications in 2013,” Ann. Nucl. Energy, 82, 142–150, 2015.
[6] D. Hwang, S. Kim, and Y. Lee, “Preliminary Analysis on the Chemical Forms of Fission Products in Nuclear Fuel via Coupling of Serpent 2 and GEMS,” *Transactions of the Korean Nuclear Society Autumn Meeting*, Changwon, Korea, Oct. 29–31, Korean Nuclear Society, 2025.
[7] D. A. Kulik, T. Wagner, S. V. Dmytrieva, G. Kosakowski, F. F. Hingerl, K. V. Chudnenko, and U. Berner, “GEM-Selektor geochemical modeling package: Numerical kernel GEMS3K for coupled simulation codes,” Computational Geosciences, Vol. 17, pp. 1–24, 2013
[8] GEMS Development Team, “GEM Task Data Structure and IPM-3 Kernel Program,” *GEMS3K Numerical kernel code* (GEM-Selektor version 3 technical documentation; Last edited: Oct. 15, 2012), 2012.
[9] I. Barin, *Thermochemical Data of Pure Substances*, 3rd ed., VCH, Weinheim; New York, 1995, DOI: 10.1002/9783527619825.
[10] GEMS specific HERACLES v.0.2 database for U, TRU and FP speciation, Paul Scherrer Institut (PSI), https://www.psi.ch/en/heracles/gems-specific-heracles-database (visited on Jan. 29, 2026).
[11] B. Simondi-Teisseire, N. Girault, F. Payot, and B. Clément, “Iodine behaviour in the containment in Phébus FP tests,” *Ann. Nucl. Energy*, 61, 157–169, 2013.
[12] K. Minato, “Thermodynamic analysis of cesium and iodine behavior in severe light water reactor accidents,” J. Nucl. Mater., 185(2), 154–158, 1991.
[13] M. Gouëllo, A. Cousin, V. Sopinskyy, and S. Bechta, “Revaporization Behavior of Cesium and Iodine Compounds from Their Deposits in the Steam–Boron Atmosphere,” ACS Omega, 6, 34016–34025, 2021.
[14] K. Ross, J. Phillips, R. O. Gauntt, and K. C. Wagner, “MELCOR Best Practices as Applied in the State-of-the-Art Reactor Consequence Analyses (SOARCA) Project,” NUREG/CR-7008, U.S. Nuclear Regulatory Commission, Washington, DC, August 2014, p. 38.